Resonance behavior for the dynamical friction of a system in a trapping potential

Ming-Gen Li and Jing-Dong Bao*
Department of Physics, Beijing Normal University, Beijing 100875, People's Republic of China

(Received 16 June 2022; accepted 14 October 2022; published 24 October 2022)

The kinetic energy fluctuation metric $\Omega_{\mathbf{K}}(t)$ is modified to extract the dynamical friction in non-Markovian scenarios to circumvent Markovian scenarios. Dynamical friction is calculated from the ratio $\Omega_{\mathbf{K}}(0)/\Omega_{\mathbf{K}}(t)$, which obeys a universal scaling law. Both analytical and numerical results of a minimal non-Markovian model substantiate the validity of the modified kinetic energy fluctuation metric. We reveal that previous studies on the rates of relaxation in harmonically bounded proteins, which are somewhat larger than those resulting from the experimental fit, may have neglected non-Markovian effects. When applying the metric to a system subjected to thermal broadband colored noise in the harmonic potential, resonance phenomenon occurs. Specifically, dynamical friction varies nonmonotonically with the frequency of the harmonic potential. The optimal frequency inducing the strongest dynamical friction matches well with the peak frequency of power spectrum of thermal broadband colored noise. The system then approaches to equilibrium rapidly. For an acoustic phonon spectrum, the resonance for dynamical friction provides further insight as to why complete thermalization only occurs when the particle frequency of the system is within a certain range of the environment particle frequencies. This is because the closer the potential frequency is to the central value of the range of frequencies, the stronger is the dynamical friction induced.

DOI: 10.1103/PhysRevResearch.4.043058

I. INTRODUCTION

Friction plays an important role in describing the dissipative effects in protein dynamics [1,2], multidimensional fission [3,4], and, most notably, phase transitions [5,6]. At the macroscopic level, the viscous Stokes friction is related to the dissipative force $F_{\mathbf{diss}} = -m\gamma_0 v$ felt by a particle of mass m moving with velocity v; here, γ_0 denotes the coefficient of static friction [7]. At a microscopic level, friction is still poorly understood [8]. Feynman argued that with an atomic perspective friction originates from two nonflat surfaces in contact with each other [9]. Friction is fundamentally described through a generalized Langevin equation (GLE) model that reflects the dissipative effects of a bath on the detailed dynamics of a system [10–12]. Because of the great significance of friction in many scientific areas of physics, chemistry, and biophysics, the task of understanding the physics of friction has acquired immense popularity [13–17].

Recently, through a Langevin dynamical model, a mechanism underlying friction was extracted using a method for computing the rate of kinetic energy relaxation that makes use of the kinetic metric of the ergodic measure [18,19]. In Markovian scenarios, the method not only provides a direct and accurate means of quantifying friction, but has also been successfully applied to collisions and activated barrier crossings in proteins [20,21]. However, the Markovian approximation is only an idealization in many instances and is inaccessible to an experimentalist [22]. Memory effects are important in systems of mesoscopic scale [23,24], especially protein folding [25–27] and self-seeding or self-nucleation during polymer crystallization [28]. Although it is in principle possible to estimate friction through the Einstein relation for the translational diffusion constant $D = k_B T/m\gamma_0$ [29], the task is very difficult because of the length scales (1–10 Å) and time scales (0.1 ps–1 ns) for thermal relaxation processes in proteins. We have developed a modified kinetic energy fluctuation metric for extracting dynamical friction in non-Markovian scenarios. Friction in this situation has a "memory"that depends on the velocity history, which implies that the rate of kinetic energy relaxation is strongly dependent on the intrinsic correlation time of the noise source [30].

With a minimal non-Markovian model in terms of the GLE driven by Ornstein–Uhlenbeck noise, the validity of the modified kinetic energy fluctuation metric is verified. We show that our results are consistent with that from the Einstein relation, whereas the unmodified metrics fail completely. Non-Markovian effects may account for deviations in the rates of relaxation in proteins obtained in previous studies and from experimental fits [19]. When we apply the metric to a system subjected to thermal broadband colored noise [31] in a harmonic potential, the resonance phenomenon is revealed [32–34]. Dynamical friction acting on the system varies nonmonotonically with the frequency of the harmonic potential. Correspondingly, the system exhibits fast thermalization. The resonancelike phenomenon seen in acoustic phonon spectra [35–37] provides further insight as to why

*jdbao@bnu.edu.cn

complete thermalization only occurs within a certain range of frequencies [38].

Our paper is structured as follows. In Sec. II, we develop the modified kinetic energy fluctuation metric. Adopting a generalized Langevin model, we calculate analytically and numerically the dynamical friction for a minimal non-Markovian model. We also compare Markovian and minimal non-Markovian Langevin models of the dynamics of proteins. In Sec. III, we investigate the resonance phenomenon that occurs in a system subjected to thermal broadband colored noise in a harmonic potential. The results also help our understanding of the occurrence of complete thermalization within a certain range of frequencies. The last section presents our conclusions.

II. MEASURE OF DYNAMICAL FRICTION

In Markovian scenarios, the delta function in time indicates that there is no correlation between impacts in any distinct time intervals dt and ds. Specifically, the intrinsic correlation time of a noise source has no influence on kinetic energy relaxation. However, for non-Markovian scenarios, the time-dependent friction function may depend on the velocity history $v(s)$ for times s that are earlier than times t. Thus, for any colored noise, which implies a significant deviation from Markovian behavior, the effect of the intrinsic correlation time of a noise source on dynamical friction should be taken into consideration.

A. Modified Kinetic energy fluctuation metric

We consider a modified kinetic energy fluctuation metric, $\Omega_{\mathbf{K}}(t)$, to determine dynamical friction in non-Markovian scenarios. $\Omega_{\mathbf{K}}(t)$ may be written as

$$\Omega_{\mathbf{K}}(t) = \frac{1}{t^2}\int_0^t\int_0^t C_{\mathbf{K}}(t_1 - t_2)\,dt_1 dt_2 - C_{\mathbf{K}}(0)\frac{\tau_\xi}{t}, \quad (1)$$

where the function $C_{\mathbf{K}}(t_1 - t_2)$ is the equilibrium autocorrelation function for the fluctuations in the kinetic energy. The parameter τ_ξ denotes the intrinsic correlation time of the noise source $\xi(t)$ [30],

$$\tau_\xi = \frac{\int_0^\infty |\langle \xi(t)\xi(0)\rangle| dt}{\langle \xi^2(0)\rangle}. \quad (2)$$

There are a few theoretical papers which consider the universal scaling law of the metric, $\Omega_{\mathbf{K}}(0)/\Omega_{\mathbf{K}}(t)$ [18,19,39]. We assume that the decay of Eq. (1) is governed by a single parameter $\gamma_{\mathbf{dyn}}$ associated with dynamical friction [19] and consider the inverse ratio

$$F[\gamma_{\mathbf{dyn}}t] \equiv \frac{\Omega_{\mathbf{K}}(0)}{\Omega_{\mathbf{K}}(t)} = \frac{1}{2\int_0^\infty C_v(y)^2\,dy - \tau_\xi}\,t, \quad (3)$$

where $\Omega_{\mathbf{K}}(0) = C_{\mathbf{K}}(0)$ is evaluated from Eq. (1) by applying $\frac{0}{0}$-type Hôpital's rule and the velocity autocorrelation function (VACF), $C_v(y) \equiv \langle v(y)v(0)\rangle/\langle v^2(0)\rangle$. It follows that

$$\gamma_{\mathbf{dyn}} = \mathbf{slope}\left[\frac{\Omega_{\mathbf{K}}(0)}{\Omega_{\mathbf{K}}(t)}\right] = \frac{1}{2\int_0^\infty C_v(y)^2\,dy - \tau_\xi}. \quad (4)$$

Details of the derivation of Eqs. (3) and (4) can be seen in Appendix A. Using the modified kinetic energy fluctuation metric, dynamical friction acting on the system may be determined not only from the Langevin dynamical model, but also from the generalized Langevin dynamical model.

Note that when $\tau_\xi = 0$ (Markovian scenario), Eq. (4) is reduced safely to the results of the unmodified metric. Dynamical friction extracted from the unmodified metric is defined by $\Gamma_{\mathbf{dyn}} \equiv 1/(2\int_0^\infty C_v(y)^2 dy)$ [19]. At the microscopic level, friction describes the dissipative effects of a general bath on the dynamics of a well-defined system, which originates from the stochastic motion of oscillators in the bath. Thus, memory effects imposing on the dynamics friction of the system are supposed to be considered. Although dynamics friction can be evaluated exactly from the unmodified metric in the Markovian case, the validity of the modified metric is verified below with a minimal non-Markovian model ($\tau_\xi \neq 0$).

B. Evaluation of $\gamma_{\mathbf{dyn}}$ for generalized Langevin equation models

The present model is established in the GLE originating from the system-plus-heat bath model [40,41]. The generalized Brownian motion of a particle with mass m in a potential $U(x)$ is described by the following GLE [10–12]:

$$m\dot{v}(t) = -m\int_0^t \gamma(t-s)v(s)ds - U'(x) + \xi(t), \quad (5)$$

where the zero-mean noise $\xi(t)$ is represented by a function of the initial position and velocities of the bath variables, and $\gamma(t-s)$ denotes the memory function. Their relationship is underscored by the fluctuation–dissipation theorem [42]: $\langle \xi(t)\xi(s)\rangle = mk_{\mathrm{B}}T\gamma(t-s)$; here, k_{B} denotes the Boltzmann constant and T the temperature. The dot $(\cdot)$ and prime $(')$ symbols signify the first derivatives with respect to time (t) and space (x), respectively.

In the absence of an external potential, i.e., $U(x) = 0$, we use the initial velocity $v(0)$ to multiply Eq. (5) and perform the ensemble average. The integral-differential equation for the VACF is given by

$$\frac{dC_v(t)}{dt} = -\int_0^t dt_1\,\gamma(t-t_1)C_v(t_1). \quad (6)$$

If the memory kernel is a delta function $\gamma(t-s) = 2\gamma_0\delta(t-s)$, the VACF may be solved analytically, which is given by $C_v(t) = \exp(-\gamma_0 t)$. Note that the modified kinetic energy fluctuation metric reduces to the unmodified metric because $\tau_\xi = 0$. Aided by Eq. (4), we obtain $\gamma_{\mathbf{dyn}} = \gamma_0$.

To investigate quantitatively the role of the intrinsic correlation time of the noise source, we consider a minimal non-Markovian model that obeys a GLE with memory kernel $\gamma(t) = \gamma_0\Omega\exp(-\Omega t)$, where $\Omega = 1/\tau_c$. The Laplace transform of the VACF reads $\hat{C}_v(z) = 1/[z + \hat{\gamma}(z)]$, in which the Laplace transform of the memory kernel is given by $\hat{\gamma}(z) = \gamma_0\Omega/(z+\Omega)$. Applying the residue theorem [43], we obtain an expression for the VACF [44], $C_v(t) =$

$$\begin{cases} \frac{1}{2\sqrt{\triangle}}\left[A\exp\left(-\frac{B}{2}t\right) - B\exp\left(-\frac{A}{2}t\right)\right]; & \triangle > 0, \\ \left[\frac{\Omega}{2}t + 1\right]\exp\left(-\frac{\Omega}{2}t\right); & \triangle = 0, \\ \frac{\exp(-\frac{\Omega t}{2})}{\sqrt{-\triangle}}\left[\sqrt{-\triangle}\cos\left(\frac{\sqrt{-\triangle}t}{2}\right) + \Omega\sin\left(\frac{\sqrt{-\triangle}t}{2}\right)\right]; & \triangle < 0, \end{cases} \quad (7)$$

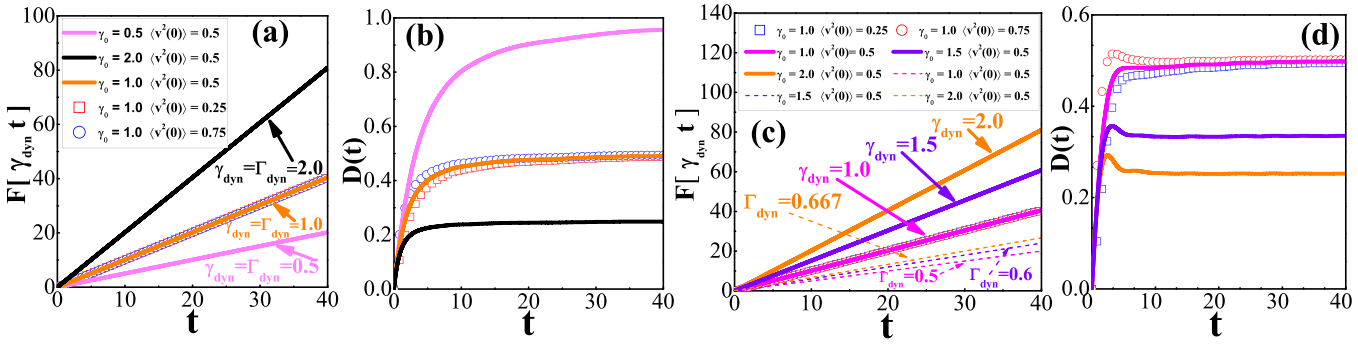

FIG. 1. Time-dependent universal function F and diffusion coefficient $D(t)$ in the two scenarios: Markovian [panels (a) and (b)] and minimal non-Markovian [panels (c) and (d)]. Data points are taken from Monte Carlo simulations of Eq. (5) with time step 10^{-3} and 10^5 trajectories. $\Gamma_{\mathbf{dyn}}$ denotes the dynamical friction obtained from the unmodified metric. The parameter settings used are $m = 1.0$, $k_BT = 0.5$, and $\Omega = 1.0$.

where $\triangle = \Omega^2 - 4Q$, $Q = \gamma_0\Omega$, $A = \Omega + \sqrt{\triangle}$, and $B = \Omega - \sqrt{\triangle}$. Hence,

$$\gamma_{\mathbf{dyn}} = \frac{1}{2\int_0^\infty C_v(y)^2\,dy - \tau_\xi} = \gamma_0, \tag{8}$$

where $\tau_\xi = 1/\Omega$ has been used; details of the derivations are provided in Appendix B.

In Fig. 1, we plot the time-dependent universal function F and diffusion coefficient $D(t)$ in the two scenarios: the Markovian and minimal non-Markovian. Diffusion coefficient $D(t) \equiv \langle x^2(t)\rangle/2t$, where $\langle x^2(t)\rangle$ is the mean-squared displacement of the system. Data points are taken from Monte Carlo simulations of Eq. (5). Details of the simulations are given in Appendix C. Notably, dynamical friction extracted through the modified kinetic energy fluctuation metric is consistent with that obtained from the Einstein relation $D = k_BT/m\gamma_0$, where $\gamma_0 = \int_0^\infty \gamma(t)dt$. Figures 1(a) and 1(c) also depict the extracted dynamical friction with different initial velocity preparations. We find the results are independent of the prepared initial conditions. In Fig. 1(c), we compared the universal function F with the unmodified metric. Clearly, the unmodified metric fails to extract the dynamical friction when non-Markovian effects are considered.

C. Protein friction: Comparison of Markovian and minimal non-Markovian Langevin models

There are several experimental techniques, including time-resolved infrared spectroscopy, reaction kinetics experiment, and resonance Raman spectroscopy [45–47], which measure frictional forces acting upon a system. One direct experimental probe of friction in proteins is through quasielastic neutron scattering [48]. Reference [19] demonstrates that relaxation times for local fluctuations fall within 1–10 ps^{-1} using a computation method for the rate of kinetic energy relaxation described by a Markovian Langevin dynamical model. However, the rates of relaxation are somewhat larger than those resulting from experimental fits interpreted by Langevin normal mode models, specifically, 0.90 ps^{-1} and 0.45 ps^{-1}. The discrepancy may have arisen in part because the experimental fits were dominated by low-temperature data.

In this work, we found that neglecting non-Markovian effects in the kinetics of protein dynamics may cause the deviation. Special systems may exist that behave in a Markovian way, in principle, but for example, transition path times reveal non-Markovian effects in the dynamics of protein folding [25–27]. On imposing a harmonic potential, i.e., $U(x) = \frac{1}{2}m\omega_0^2x^2$, we compared the dynamical friction extracted from the Markovian Langevin model with that from the minimal non-Markovian model. We obtain a differential equation for the VACF,

$$\frac{dC_v(t)}{dt} = -\int_0^t \left[\gamma(t-t_1) + \omega_0^2\right]C_v(t_1)\,dt_1. \tag{9}$$

For the Markovian scenario, we obtain $C_v(t) = \exp(-\gamma_0 t/2)[\cos(at) - \gamma_0/2a\sin(at)]$, for which $a = \omega_0^2 - \gamma_0^2/4$. One obtains $\gamma_{\mathbf{dyn}} = \gamma_0$ with $\tau_\xi = 0$. Although no closed form has been found for the minimal non-Markovian scenario, we can achieve accurate evaluations using numerical methods (see Appendix C). In Fig. 2(a), we plot the frequency dependence of dynamical friction computed from Markovian and minimal non-Markovian Langevin dynamic models. When non-Markovian effects are taken into account, dynamical friction is substantially smaller than that obtained from the Markovian model. We thus infer that memory effects in which the time-dependent friction function depends on the velocity history lead to slow relaxation of the system. Correspondingly, relaxation rates become small. When the intrinsic correlation time $\tau_\xi = 1/\Omega$ of the noise source becomes long, memory effects are more pronounced and dynamical friction decays fast [Fig. 2(a)]. For long intrinsic correlation times, effects of the external potential acting on the system are weaker due to pronounced memory effects. The system approaches its equilibrium state slowly and the corresponding dynamical friction becomes weaker. When effects of the external potential disappear ($\omega_0 \to 0$), dynamical friction in protein friction is reduced to the result of Eq. (8) in Sec. II B.

In order to provide a further understanding that non-Markovian effects might also account for the phenomenon that the previous studies on the rates of relaxation in proteins are somewhat larger than those resulting from the experimental fit, we compare dynamical friction extracted from various evaluated methods in Fig. 2(b). As a practical example, we analyze dynamical friction $\gamma_{\mathbf{dyn}} = 0.90\ \text{ps}^{-1}$ that resulted in the best fit to the experimental data in the parametrization [48].

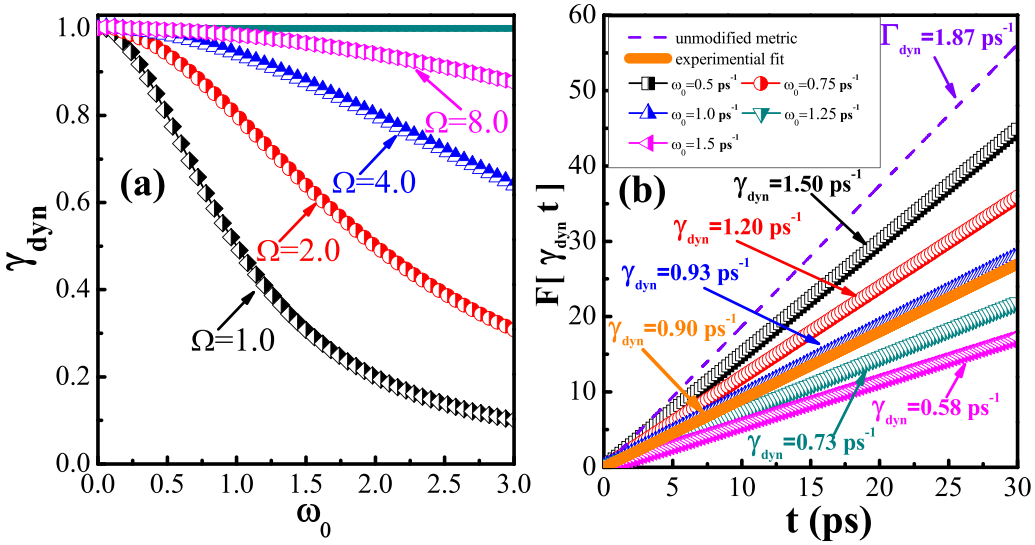

FIG. 2. (a) Dynamical friction $\gamma_{\mathbf{dyn}}$ vs harmonic potential frequency ω_0. Solid line and colored symbols denote Markovian and minimal non-Markovian process, respectively. The parameter $\gamma_0 = 1.0$ is used. (b) Time-dependent universal function F with various evaluated methods in a practical example: unmodified metric, experimental fit, and modified metric (colored symbols). The parameters $\gamma_0 = 1.87$ $\mathbf{ps}^{-1}$ and $\Omega = 1.0$ $\mathbf{ps}^{-1}$ are used. Date points are calculated numerically from Eq. (9).

With the unmodified metric, it has been found that dynamical friction falls on the order of 1–10 ps^{-1}, specifically, $\gamma_{\mathbf{dyn}} = 1.87$ ps^{-1} (see Fig. 2 of Ref. [19]), which is independent of harmonic potential frequency ω_0. Setting $\gamma_0 = 1.87$ ps^{-1} and $\Omega = 1.0$ ps^{-1} in the minimal non-Markovian model, we can find that dynamical friction gradually approaches the value of experimental fit in Fig. 2(b) with ω_0 increasing. Thus, the derivation of dynamical friction between the unmodified metric and experimental fit may be reconciled by considering non-Markovian effects due to the complexity of the cell's internal environment [49].

III. RESONANCE OF DYNAMICAL FRICTION

A. Thermal broadband colored noise

We apply the modified kinetic energy fluctuation metric to a system subjected to thermal broadband colored noise [31], thereby allowing a coverage from "red" noise to "green" noise [50,51] associated with a memory kernel [52,53]; specifically,

$$\gamma(t) = \Gamma_0\left[\frac{1}{\tau_2}\exp\left(-\frac{t}{\tau_2}\right) - \frac{1}{\tau_1}\exp\left(-\frac{t}{\tau_1}\right)\right], \qquad (10)$$

with $\Gamma_0 = \gamma_0\tau_1^2/(\tau_1^2 - \tau_2^2)$, where τ_1 and τ_2 denote two correlation times of two Ornstein–Uhlenbeck noises. It is worth noticing that the spectrum of noise introduced here varies nonmonotonically with the frequency [Eq. (12)]. This could stem from the complexity of the cell's internal environment [49]. Indeed, this noise can be realized from the difference between two Ornstein–Uhlenbeck noises with different time constants driven by the same white noise. Under force-free conditions, the ballistic behavior is expected to emerge, as evident in Fig. 3(a). This behavior arises because the effective friction vanishes in the long-time limit, i.e., $\lim_{t\to\infty}\int_0^t \gamma(t - t_1)dt_1 = 0$. The result is also verified using the modified kinetic energy fluctuation metric.

After a straightforward derivation, the VACF is given by

$$\begin{aligned} C_v(t) = {} & h/(h+f) + \exp(-gt/2)[\cos(kt) \\ & + g/2k\sin(kt)] - h/[k(h+f)]\exp(-gt/2) \\ & \times [g/2\sin(kt) + k\cos(kt)], \end{aligned} \qquad (11)$$

where $g = (\tau_1 + \tau_2)/(\tau_1\tau_2)$, $h = 1/(\tau_1\tau_2)$, $f = \Gamma_0(\tau_1 - \tau_2)/(\tau_1\tau_2)$, and $k = \sqrt{h + f - g^2/4}$. In the long-time limit, the VACF approaches a nonzero value, i.e., $\lim_{t\to\infty} C_v(t) = h/(h+f)$, which is also observed in Fig. 3(b). We inferred that $1/(2\int_0^\infty C_v(y)^2\,dy - \tau_\xi) \to \infty$, on setting $\tau_\xi = 0$, and thus $\gamma_{\mathbf{dyn}} = 0$.

We next investigate how dynamical friction responds to external harmonic potential. Unfortunately, no closed form has been found for the time domain function in Eq. (9) with Eq. (10). However, numerical methods again yield accurate evaluations. For Fig. 4(a), we calculated the dynamical

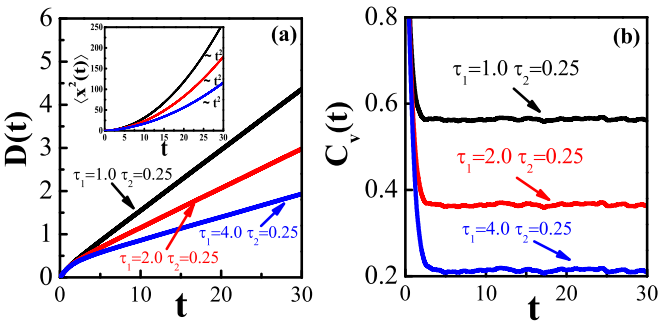

FIG. 3. Time-dependence of the coefficient of diffusion $D(t)$ and VACF $C_v(t)$ with various τ_1 and τ_2 for a system subjected to a thermal broadband colored noise under force-free conditions. The inset shows the behavior of the time-dependent mean-squared displacement $\langle x^2(t)\rangle$. The parameter settings are those of Fig. 1 along with $\gamma_0 = 1.0$.

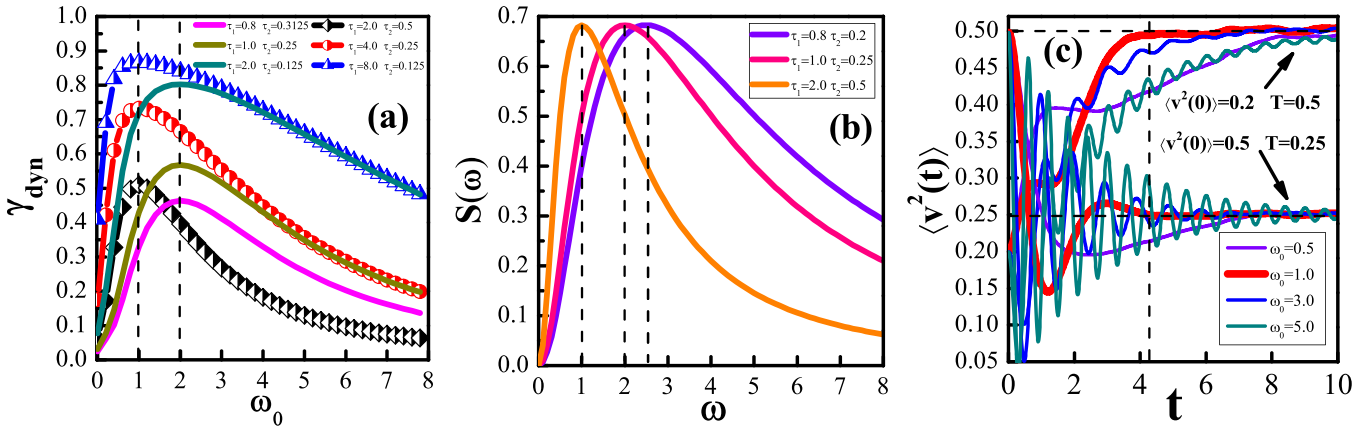

FIG. 4. (a) Dynamical friction $\gamma_{\mathbf{dyn}}$ vs harmonic potential frequency ω_0 for the system subjected to thermal broadband colored noise with various τ_1 and τ_2 values. Data points are calculated numerically using Eq. (9) with Eq. (10). (b) Power spectrum of thermal broadband colored noise for various τ_1 and τ_2. (c) Time-dependent mean-squared velocity $\langle v^2(t)\rangle$ for the system for different initial condition preparations, various ω_0, and fixed $\tau_1 = 4.0$ and $\tau_2 = 0.25$. Data points are from Monte Carlo simulations for Eq. (5) with a time step of 10^{-3} and 10^5 trajectories; the setting $\gamma_0 = 1.0$ is used.

friction $\gamma_{\mathbf{dyn}}$ for various frequencies of the harmonic potential ω_0; we find that it varies nonmonotonically with ω_0. The optimal frequency, which induces the strongest dynamical friction, matches the peak frequency of power spectrum of the thermal broadband colored noise. According to the Wiener–Khintchine theorem [54], the spectral density of noise is the Fourier transformation of the correlation function of noise,

$$S(\omega) = k_B T \frac{2\Gamma_0 \tau_1^2 \omega^2}{\left(1+\tau_1^2\omega^2\right)\left(1+\tau_2^2\omega^2\right)}. \tag{12}$$

By calculating $dS(\omega)/d\omega = 0$, the peak of the power spectrum is found to be at $\omega_p = 1/\sqrt{\tau_1\tau_2}$. In Fig. 4(b), we plot the spectral density of noise $J(\omega)$ for various parameter values of τ_1 and τ_2.

In other words, resonance phenomenon occurs when the thermal broadband colored noise responds to an external potential. Dynamical friction is strengthened if the frequency ω_0 of the harmonic potential nears the peak frequency ω_p of the power spectrum. Setting $\tau_1 = 4.0$ and $\tau_2 = 0.25$, we also plot the variance of the velocity $\langle v^2(t)\rangle$ for the particle in a harmonic potential for various potential frequencies in Fig. 4(c). The variance of the velocity approaches an equilibrium value because of the confining potential. However, fast thermalization appears when resonance phenomenon occurs. Specifically, $\langle v^2(t)\rangle$ rapidly approaches an equilibrium value $k_B T$, and the relaxation time is shortened when the frequency of the potential ω_0 nears ω_p. When dynamical friction becomes stronger, the frequency of the energy exchange between system and environment is faster. Finally, the system approaches its equilibrium quickly.

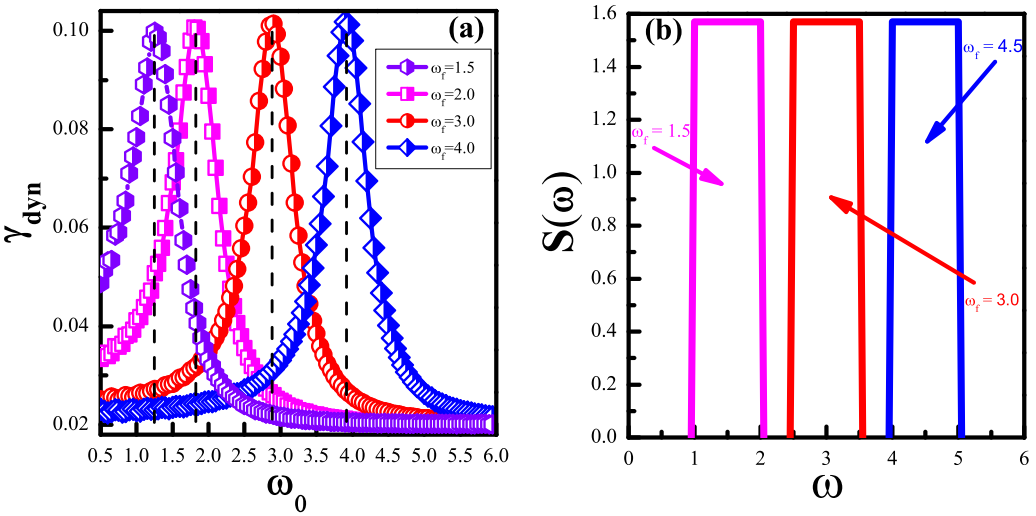

FIG. 5. (a) Dynamical friction $\gamma_{\mathbf{dyn}}$ vs harmonic potential frequency ω_0 for a system subjected to noise with a long-wavelength limit for acoustic phonons but zero weight at low frequencies. Data points are calculated numerically using Eq. (9) with Eq. (13). (b) Acoustic phonons spectrum with various ω_f. The parameter settings used are $\gamma_0 = 1.0$ and $\Omega_0 = 1.0$.

B. Acoustic phonons spectrum

A few studies have found that complete thermalization in a harmonic potential only occurs when the particle frequency of the system is within a certain range of the particle frequencies of the environment [35–37]. The results reported there find wide application, encompassing systems as diverse as classical plasmas and self-gravitating objects [55], ultracold trapped atoms [56], and quasiparticles in nanostructures [57]. Therefore, further light needs to be shed on this phenomenon.

Here, the noise density of states is chosen to be $S(\omega) = W$ for $\omega_f - \Omega_0/2 \leqslant \omega \leqslant \omega_f + \Omega_0/2$ and $S(\omega) = 0$ otherwise; here, $W = \pi m k_B T \gamma_0/\Omega_0$. It originates from the long-wavelength limit of the acoustic phonons and cuts off at low frequency. Aided by the modified kinetic energy fluctuation metric, dynamical friction for various potential frequencies may be extracted. Through the nonmonotonic trend of dynamical friction, we provide a further explanation as to why complete thermalization only occurs within a certain range of frequencies in this system.

Given the fluctuation dissipation theorem, we obtain the memory kernel function [58], which has also been successfully used in disordered systems [59]; specifically,

$$\gamma(t) = \gamma_0 \frac{\sin\left(\frac{1}{2}\Omega_0 t\right)}{\frac{1}{2}\Omega_0 t} \cos(\omega_f t). \tag{13}$$

In Fig. 5, we plot the dynamical friction $\gamma_{\mathbf{dyn}}$ for various harmonic potential frequencies ω_0. Clearly, the dynamical friction $\gamma_{\mathbf{dyn}}$ varies nonmonotonically with frequency ω_0 of the harmonic potential. The nearer ω_0 is to ω_f, the center value of the range of frequencies, the stronger the dynamical friction induced. As expected, for an environment composed of many oscillators, the energy is transferred from the system to the environment [60]. When dynamical friction becomes strong, the frequency of the energy exchange quickens, and consequently, complete thermalization occurs.

IV. CONCLUSION

To achieve a reliable application in non-Markovian scenarios, the kinetic energy fluctuation metric has been modified. With a minimal non-Markovian model, we have verified the validity of the modified kinetic energy fluctuation metric analytically and numerically. The extracted dynamical friction is consistent with that obtained from the Einstein relation, whereas the unmodified metric fails entirely. Under the influence of a harmonic potential, the deviation seen in previous studies for the rates of relaxation are somewhat larger than those from the experimental fits and may have arisen because non-Markovian effects on the kinetics of protein dynamics were neglected. We have revealed that a system subjected to thermal broadband colored noise exhibits resonance behavior; specifically, dynamical friction varies nonmonotonically with the frequency of the harmonic potential. Fast thermalization occurs when the potential frequency matches the peak frequency of the power spectrum of colored noise because dynamical friction is strongest in this situation. By employing an acoustic phonon spectrum, further insight into a complete thermalization was obtained.

We performed a detailed study of the modified kinetic energy fluctuation metric, which has been applied successfully to classical bounded Markovian and non-Markovian systems. Although the metric for extracting dynamical friction remains an open topic, further study may reveal other surprising findings when these systems are unbounded [61] and extended to quantum scenarios [62].

ACKNOWLEDGMENT

This work was supported by the National Natural Science Foundation of China under Grant No. 11735005.

APPENDIX A: DERIVATIONS OF EQS. (3) AND (4)

For equilibrium correlation functions, there is no preferred origin of time and thus $C_{\mathbf{K}}(t_1 - t_2)$ can only depend on $|t_1 - t_2|$. Under these circumstances, Eq. (1) may be rewritten as

$$\Omega_{\mathbf{K}}(t) = \frac{2}{t^2}\int_0^t (t-y)\, C_{\mathbf{K}}(y)\, dy - C_{\mathbf{K}}(0)\frac{\tau_\xi}{t}, \tag{A1}$$

where the function $C_{\mathbf{K}}(t)$ is given by

$$C_{\mathbf{K}}(t) = \frac{m^2}{4}[\langle v^2(t)v^2(0)\rangle - \langle v^2(t)\rangle\langle v^2(0)\rangle]. \tag{A2}$$

Using the ensemble-average property of a Gaussian random variable $R(t)$ [63], i.e., $\langle R^2(t_1)R^2(t_2)\rangle = 2\langle R(t_1)R(t_2)\rangle^2 + \langle R^2(t_1)\rangle\langle R^2(t_2)\rangle$, we obtain $C_{\mathbf{K}}(t) = m^2/2\langle v(t)v(0)\rangle^2$. Applying the long-time limit,

$$\Omega_{\mathbf{K}}(t) = \frac{m^2}{t}\int_0^\infty \langle v(y)v(0)\rangle^2\, dy - C_{\mathbf{K}}(0)\frac{\tau_\xi}{t}. \tag{A3}$$

Substituting the above equation into Eqs. (3) and (4), the key result of this paper is derived.

APPENDIX B: DETAILS OF THE DERIVATIONS OF EQS. (7) AND (8)

Substituting $\hat{\gamma}(z) = \gamma_0\Omega/(z+\Omega)$ into $\hat{C}_v(z) = 1/[z + \hat{\gamma}(z)]$ yields

$$\hat{C}_v(z) = \frac{z+\Omega}{z^2 + \Omega z + Q}, \tag{B1}$$

where $Q = \gamma_0\Omega$. $C_v(t)$ as a key quantity can be obtained by the inverse Laplace transform of $\hat{C}_v(z)$,

$$C_v(t) = \frac{1}{2\pi i}\int_{c-i\infty}^{c+i\infty} \hat{C}_v(z)\exp(zt)dz. \tag{B2}$$

The contour for evaluating the above integral is given in Ref. [64] and the residue theorem may be used to calculate this integral fully,

$$C_v(t) = \sum_{k=1}^{2K} \mathbf{res}[\hat{C}_v(z_k)]\exp(z_k t), \tag{B3}$$

where c denotes a positive constant and z_k a root of the characteristic equation $z^2 + \Omega z + Q = 0$. Applying the residue

theorem, we obtain an expression for the VACF, $C_v(t) =$

$$\begin{cases} \frac{1}{2\sqrt{\triangle}}\left[A\exp\left(-\frac{B}{2}t\right) - B\exp\left(-\frac{A}{2}t\right)\right]; & \triangle > 0. \\ \left[\frac{\Omega}{2}t + 1\right]\exp\left(-\frac{\Omega}{2}t\right); & \triangle = 0. \\ \frac{\exp\left(-\frac{\Omega t}{2}\right)}{\sqrt{-\triangle}}\left[\sqrt{-\triangle}\cos\left(\frac{\sqrt{-\triangle}t}{2}\right) + \Omega\sin\left(\frac{\sqrt{-\triangle}t}{2}\right)\right]; & \triangle < 0. \end{cases} \tag{B4}$$

where $\triangle = \Omega^2 - 4Q$, $A = \Omega + \sqrt{\triangle}$, and $B = \Omega - \sqrt{\triangle}$; thus, we have

$$2\int_0^\infty C_v(y)^2\,dy = \frac{1}{\gamma_0} + \frac{1}{\Omega}. \tag{B5}$$

The integral result is safely retained in all three situations. From Eq. (2) with $\langle\xi(t)\xi(0)\rangle = mk_BTQ\exp(-\Omega t)$, we have

$$\tau_\xi = \frac{\int_0^\infty |\langle\xi(t)\xi(0)\rangle|dt}{\langle\xi^2(0)\rangle} = \frac{1}{\Omega}. \tag{B6}$$

Using Eqs. (B5) and (B6), we finally obtain

$$\gamma_{\mathbf{dyn}} = \frac{1}{2\int_0^\infty C_v(y)^2\,dy - \tau_\xi} = \gamma_0. \tag{B7}$$

APPENDIX C: MONTE-CARLO SIMULATIONS OF EQ. (5) AND NUMERICAL METHODS TO EVALUATE EQ. (9)

The GLE for a particle of mass m in a potential reads

$$m\dot{v}(t) = -m\int_0^t \gamma(t-s)v(s)ds - U'(x) + \xi(t), \tag{C1}$$

where $\xi(t)$ is a zero-mean Gaussian colored noised with the fluctuation–dissipation theorem: $\langle\xi(t)\xi(s)\rangle = mk_{\mathrm{B}}T\gamma(t-s)$. By using the second-order stochastic Runge–Kutta method [65] to solve Eq. (C1), the key point is the noise sequences $\xi(t)$.

In the ω-Fourier space, the noise correlation function reads

$$\langle\xi(\omega)\xi(\omega')\rangle = 2\pi mk_{\mathrm{B}}T\gamma(\omega)\delta(\omega+\omega'), \tag{C2}$$

where $\xi(\omega)$ and $\gamma(\omega)$ are the Fourier transforms of $\xi(t)$ and $\gamma(t)$, respectively. By discretizing time in $N = 2^n$ intervals of the mesh size Δt, we get the discrete version of Eq. (C2) with $\omega = 2\pi\omega_\mu/(N\Delta t)$,

$$\langle\xi(\omega_\mu)\xi(\omega_\nu)\rangle = mk_{\mathrm{B}}T\gamma(\omega_\mu)N\Delta t\delta_{\mu+\nu,0}. \tag{C3}$$

Then the noise in the Fourier space is given by

$$\begin{aligned} \xi(\omega_\mu) &= \sqrt{mk_{\mathrm{B}}TN\Delta t\gamma(\omega_\mu)}\alpha_\mu, \quad \mu = 1,\ldots,N-1 \\ \xi(\omega_0) &= \gamma(\omega_N), \end{aligned} \tag{C4}$$

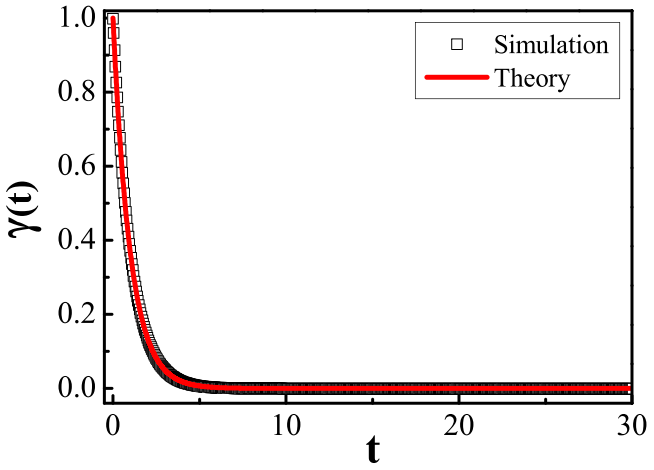

FIG. 6. Correlation function of Ornstein–Uhlenbeck noise. The black symbol signifies Monte Carlo simulation data; the red line signifies theoretical values. The parameter settings used are $m = 1.0$, $k_BT = 0.5$, $\gamma_0 = 1.0$, $\Omega = 1.0$, and $N = 2^{13}$.

where α_μ are Gaussian random numbers with zero mean and correlation $\langle\alpha_\mu\alpha_\nu\rangle = \delta_{\mu,-\nu}$. α_μ can be constructed as

$$\alpha_0 = a_0; \quad \alpha_\mu = \frac{1}{\sqrt{2}}(a_\mu + ib_\mu) \tag{C5}$$

where a_μ and b_μ are, respectively, real and imaginary parts, which are normal Gaussian random numbers. Finally, one can obtain the discrete noise $\xi(\omega_\mu)$ and $\xi(t)$ is given by inverse Fourier transform [65]. As the noise sequence has been given, the second-order stochastic Runge–Kutta method is appropriate to solve the GLE. For validation, we compared the noise correlation function, $\gamma(t) = \gamma_0\Omega\exp(-\Omega t)$, evaluated numerically from $\gamma(t_i) = \frac{1}{N_t}\sum_{j=0}^{N_t}\langle\xi(t_i + j\Delta t)\xi(t_i)\rangle$, with its theoretical value. The two results are in agreement (see Fig. 6).

Figure 2 is constructed by numerical simulation of Eq. (9), which is an integral-differential equation for $C_v(t)$. A second-order Runge–Kutta algorithm is

$$\begin{aligned} K_1 &= -\Delta t * \mathbf{Int}[C_v(\Delta t)] \\ K_2 &= -\Delta t * \mathbf{Int}[C_v(\Delta t) + \Delta t * K_1] \\ C_v(\Delta t) &= C_v(0) + 0.5\Delta t(K_1 + K_2), \end{aligned} \tag{C6}$$

where $C_v(0) = 1$ and $\mathbf{Int}[C_v(\Delta t)]$ denotes trapezoid rule for the integral on the right of Eq. (9). Then time series of $C_v(t)$ can be obtained and dynamical friction $\gamma_{\mathbf{dyn}}$ is evaluated from Eq. (4).

[1] J. E. Straub and D. Thirumalai, Exploring the energy landscape in proteins, Proc. Natl. Acad. Sci. USA **90**, 809 (1993).

[2] D. K. Klimov and D. Thirumalai, Stretching single-domain proteins: Phase diagram and kinetics of force-induced unfolding, Proc. Natl. Acad. Sci. USA **96**, 6166 (1999).

[3] N. Takigawa and M. Abe, Thermal decay rate of multidimensional fission under a nonlinear coupling, Phys. Rev. C **41**, 2451 (1990).

[4] T. Nakatsukasa, K. Matsuyanagi, M. Matsuo, and K. Yabana, Time-dependent density-functional description of nuclear dynamics, Rev. Mod. Phys. **88**, 045004 (2016).

[5] A. Giraldo, B. Krauskopf, N. G. R. Broderick, J. A. Levenson, and A. M. Yacomotti, The driven-dissipative Bose-Hubbard dimer: Phase diagram and chaos, New J. Phys. **22**, 043009 (2020).

[6] I. Goychuk and T. Pöschel, Nonequilibrium Phase Transition to Anomalous Diffusion and Transport in a Basic Model of Nonlinear Brownian Motion, Phys. Rev. Lett. **127**, 110601 (2021).

[7] R. Zwanzig, *Nonequilibrium Statistical Mechanics* (Oxford Univesity Press, New York, 2001).

[8] L. Lin, T. R. Cui, L.-C. Qin, and S. Washburn, Direct Measurement of the Friction between and Shear Moduli of Shells of Carbon Nanotubes, Phys. Rev. Lett. **107**, 206101 (2011).

[9] R. P. Feynman, *The Feynman Lectures On Physics Volume I*, The New Millennium Edition (Basic Books, New York, 2010).

[10] R. Zwanzig, Theory of vibrational relaxation in liquids, J. Chem. Phys. **34**, 1931 (1961).

[11] H. Mori, Transport, collective motion, and Brownian motion, Prog. Theor. Phys. **33**, 423 (1965).

[12] M. H. Lee, Solutions of the generalized Langevin equation by a method of recurrence relations, Phys. Rev. B **26**, 2547 (1982).

[13] A. Vanossi, N. Manini, M. Urbakh, S. Zapperi, and E. Tosatti, *Colloquium*: Modeling friction: From nanoscale to mesoscale, Rev. Mod. Phys. **85**, 529 (2013).

[14] T. Baumberger, P. Berthoud, and C. Caroli, Physical analysis of the state- and rate-dependent friction law. II. Dynamic friction, Phys. Rev. B **60**, 3928 (1999).

[15] Y. Sang, M. Dubé, and M. Grant, Dependence of friction on roughness, velocity, and temperature, Phys. Rev. E **77**, 036123 (2008).

[16] J. D. Bao, X. R. Wang, and W. M. Liu, Ergodic time scale and transitive dynamics in single-particle tracking, Phys. Rev. E **103**, 032136 (2021).

[17] J. D. Bao, Time-dependent fractional diffusion and friction functions for anomalous diffusion, Front. Phys. **9**, 567161 (2021).

[18] D. Thirumalai and R. D. Mountain, Ergodic convergence properties of supercooled liquids and glasses, Phys. Rev. A **42**, 4574 (1990).

[19] D. E. Sagnella, J. E. Straub, and D. Thirumalai, Time scales and pathways for kinetic energy relaxation in solvated proteins: Application to carbonmonoxy myoglobin, J. Chem. Phys. **113**, 7702 (2000).

[20] P. Hänggi, P. Talkner, and M. Borkovec, Reaction-rate theory: Fifty years after Kramers, Rev. Mod. Phys. **62**, 251 (1990).

[21] R. Zwanzig, Diffusion in a rough potential, Proc. Natl. Acad. Sci. USA **85**, 2029 (1988).

[22] R. Satija, A. Das, and D. E. Makarov, Transition path times reveal memory effects and anomalous diffusion in the dynamics of protein folding, J. Chem. Phys. **147**, 152707 (2017).

[23] H. Meyer, F. Glatzel, W. Wöhler, and T. Schilling, Evaluation of memory effects at phase transitions and during relaxation processes, Phys. Rev. E **103**, 022102 (2021).

[24] N. Leibovich and E. Barkai, Infinite ergodic theory for heterogeneous diffusion processes, Phys. Rev. E **99**, 042138 (2019).

[25] E. Medina, R. Satija, and D. E. Makarov, Transition path times in non-Markovian activated rate processes, J. Phys. Chem. B **122**, 11400 (2018).

[26] R. Satija and D. E. Makarov, Generalized Langevin equation as a model for barrier crossing dynamics in biomolecular folding, J. Phys. Chem. B **123**, 802 (2019).

[27] C. Ayaz, L. Tepper, F. N. Brünig, J. Kappler, J. O. Daldrop, and R. R. Netz, Non-Markovian modeling of protein folding, Proc. Natl. Acad. Sci. USA **118**, e2023856118 (2021).

[28] X. Y. Li, F. M. Su, Y. X. Ji, N. Tian, J. Lu, Z. Wang, Z. M. Qi, and L. B. Li, Influence of the memory effect of a mesomorphic isotactic polypropylene melt on crystallization behavior, Soft Matter **9**, 8579 (2013).

[29] J. D. Bao, Generalized Einstein relations and conditions for anomalous relaxation, Phys. Rev. E **100**, 052149 (2019).

[30] P. Hänggi and P. Jung, Colored noise in dynamical systems, Adv. Chem. Phys. **89**, 239 (1995).

[31] J. D. Bao and Y. Z. Zhuo, Ballistic Diffusion Induced by a Thermal Broadband Noise, Phys. Rev. Lett. **91**, 138104 (2003).

[32] J. D. Bao, Y. L. Song, Q. Ji, and Y. Z. Zhuo, Harmonic velocity noise: Non-Markovian features of noise-driven systems at long times, Phys. Rev. E **72**, 011113 (2005).

[33] J. Ren, W.-X. Wang, and F. Qi, Randomness enhances cooperation: A resonance-type phenomenon in evolutionary games, Phys. Rev. E **75**, 045101(R) (2007).

[34] J.-H. Li and S.-G. Chen, Drift Motion, Phenomenon of Resonance, and Diffusive Motion Induced by a Chaotic Signal, Phys. Rev. Lett. **93**, 014102 (2004).

[35] R. Morgado, F. A. Oliveira, G. G. Batrouni, and A. Hansen, Relation between Anomalous and Normal Diffusion in Systems with Memory, Phys. Rev. Lett. **89**, 100601 (2002).

[36] I. V. L. Costa, R. Morgado, M. V. B. T. Lima, and F. A. Oliveira, The fluctuation-dissipation theorem fails for fast superdiffusion, Europhys. Lett. **63**, 173 (2003).

[37] M. H. Vainstein, I. V. L. Costa, R. Morgado, and F. A. Oliveira, Non-exponential relaxation for anomalous diffusion, Europhys. Lett. **73**, 726 (2006).

[38] S. T. Smith and R. Onofrio, Thermalization in open classical systems with finite heat baths, Eur. Phys. J. B **61**, 271 (2008).

[39] D. Thirumalai, R. D. Mountain, and T. R. Kirkpatrick, Ergodic behavior in supercooled liquids and in glasses, Phys. Rev. A **39**, 3563 (1989).

[40] A. O. Caldeira and A. J. Leggett, Influence of Dissipation on Quantum Tunneling in Macroscopic Systems, Phys. Rev. Lett. **46**, 211 (1981).

[41] A. O. Caldeira and A. J. Leggett, Quantum tunnelling in a dissipative system, Ann. Phys. **149**, 374 (1983).

[42] R. Kubo, M. Toda, and M. Hashitsume, *Statistical Physics II, Nonequilbrium Statistical Mechanics* (Springer, Berlin, 1985).

[43] R. Muralidhar, D. J. Jacobs, D. Ramkrishna, and H. Nakanishi, Diffusion on two-dimensional percolation clusters: Influence of cluster anisotropy, Phys. Rev. A **43**, 6503 (1991).

[44] T. Srokowski and M. Płoszajczak, Solving the generalized Langevin equation with the algebraically correlated noise, Phys. Rev. E **57**, 3829 (1998).

[45] D. W. Oxtoby, Hydrodynamic theory for vibrational dephasing in liquids, J. Chem. Phys. **70**, 2605 (1979).

[46] D. W. Oxtoby, Dephasing of molecular vibrations in liquids, Adv. Chem. Phys. **40**, 1 (1979).

[47] D. W. Oxtoby, A useful interpolation between static and motional narrowing limits for vibrational dephasing, J. Chem. Phys. **74**, 1503 (1981).

[48] J. C. Smith, Protein dynamics: Comparison of simulations with inelastic neutron scattering experiments, Q. Rev. Biophys. **24**, 227 (1991).

[49] G. D'Anna, P. Mayor, A. Barrat, V. Loreto, and F. Nori, Observing Brownian motion in vibration-fluidized granular matter, Nature **424**, 909 (2003).

[50] J. D. Bao and S. J. Liu, Broad-band colored noise: Digital simulation and dynamical effects, Phys. Rev. E **60**, 7572 (1999).

[51] S. A. Guz and M. V. Sviridov, "Green" noise in quasistationary stochastic systems, Chaos **11**, 605 (2001).

[52] M. Okamura and H. Mori, Time correlation functions in a similarity approximation for one-dimensional turbulence, Phys. Rev. E **79**, 056312 (2009).

[53] H. Mori and H. Fujisaka, Transport and entropy production due to chaos or turbulence, Phys. Rev. E **63**, 026302 (2001).

[54] A. Dechant and E. Lutz, Wiener-Khinchin Theorem for Nonstationary Scale-Invariant Processes, Phys. Rev. Lett. **115**, 080603 (2015).

[55] G. Alberti and P.-H. Chavanis, Caloric curves of classical self-gravitating systems in general relativity, Phys. Rev. E **101**, 052105 (2020).

[56] C. Chin, R. Grimm, P. Julienne, and E. Tiesinga, Feshbach resonances in ultracold gases, Rev. Mod. Phys. **82**, 1225 (2010).

[57] Y. Savich, L. Glazman, and A. Kamenev, Quasiparticle relaxation in superconducting nanostructures, Phys. Rev. B **96**, 104510 (2017).

[58] R. Zwanzig, Nonlinear generalized Langevin equations, J. Stat. Phys. **9**, 215 (1973).

[59] M. H. Vainstein, R. Morgado, F. A. Oliveira, F. A. B. F. de Moura, and M. D. Coutinho-Filho, Stochastic description of the dynamics of a random-exchange Heisenberg chain, Phys. Lett. A **339**, 33 (2005).

[60] J. Rosa and M. W. Beims, Dissipation and transport dynamics in a ratchet coupled to a discrete bath, Phys. Rev. E **78**, 031126 (2008).

[61] P.-H. Chavanis and C. Sire, Virial theorem and dynamical evolution of self-gravitating Brownian particles in an unbounded domain. I. Overdamped models, Phys. Rev. E **73**, 066103 (2006).

[62] S. F. Huelga and M. B. Plenio, Quantum stochastic resonance in electron shelving, Phys. Rev. A **62**, 052111 (2000).

[63] W. H. Deng and E. Barkai, Ergodic properties of fractional Brownian-Langevin motion, Phys. Rev. E **79**, 011112 (2009).

[64] F. Ishikawa and S. Todo, Localized mode and nonergodicity of a harmonic oscillator chain, Phys. Rev. E **98**, 062140 (2018).

[65] R. L. Honeycutt, Stochastic Runge-Kutta algorithms. I. White noise, Phys. Rev. A **45**, 600 (1992).